2013 IEEE/RSJ International Conference on
Intelligent Robots and Systems (IROS)
November 3-7, 2013. Tokyo, Japan

Development of Head Care Robot using Five-bar Closed Link Mechanism with Enhanced Head Shape Following Capability

Toshinori Hirose, Takeshi Ando, Soichiro Fujioka and Osamu Mizuno

Abstract— **We have developed a head care robot equipped with scrubbing fingers that washes hair and provides scalp cares in hospitals and care facilities to ease the burden on healthcare professionals and care workers. Our robot provides frequent hair washing and a higher Quality Of Life (QOL) to patients and others who need such nursing care. Its elemental technologies include the following: a cylindrical rack mechanism for self-aligning and a drive-force transmission from an electric motor to multiple fingers, a five-bar closed link mechanism to expand the area of the head that can be washed by extension motion, and rear pressure force control by a coordinated double arm motion to switch between supporting and washing the head. In addition, we introduce an orientation correction mechanism into our five-bar closed link mechanism to keep the end effector's contact face aligned along the head's surface. This paper presents several elemental technologies and the kinematics of a five-bar closed link mechanism and discusses the improvement of the head shape following capability using an orientation correction mechanism.**

I. Introduction

Maintaining cleanliness is a basic human need. Clean care, which maintains the cleanliness of patients and others in need of nursing care, has significance not only in physiology but also in sociology (e.g., personal maintenance or relaxation)[1][2]. In Japan, washing the hair of patients is an example of clean care that is given by healthcare professionals and care workers less frequently than is considered ideal. To address these problems, we applied robot hand technology to develop a head care robot with scrubbing fingers that resemble human fingers. This robot washes hair in hospitals and care facilities, eases the burden on healthcare professionals and care workers, and increases the quality of life for patients and others who need care.

In this paper, we report the development of our head care robot as well as the elemental technologies that allow it to gently touch a person on the head: a cylindrical rack mechanism for self-aligning and a drive-force transmission from an electric motor to multiple fingers, a five-bar closed link mechanism to expand the area of the head to be scrubbed by extension motion, and rear pressure force control by a coordinated double arm motion to switch between supporting and washing the head. In addition, we introduce an orientation correction mechanism into a five-bar closed link mechanism to keep the end effector's contact face aligned along the head's surface. This paper also presents the kinematics of a five-bar closed link mechanism and discusses the improvement of the head shape following capability using an orientation correction mechanism.

Toshinori Hirose, Takeshi Ando, Soichiro Fujioka and Osamu Mizuno are with New Business Promotion Project, Global Manufacturing Division, Panasonic Corporation, Osaka, Japan
hirose.toshinori@jp.panasonic.com
ando.takeshi@jp.panasonic.com
fujioka.soichiro@jp.panasonic.com
mizuno.osamu@jp.panasonic.com

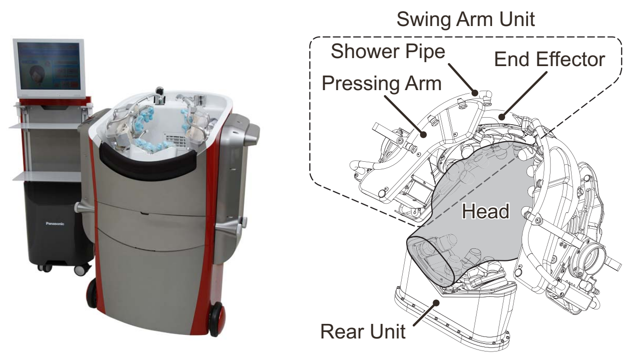

Fig. 1. Appearance and Main Composition of Head Care Robot

II. Head Care Robot

The main concept of our head care robot is to gently touch a head and shampoo it. Our head care robot produces a rich lather on a patient's head, which it lightly rubs with its fingers in much the same fashion as a beautician. Fig. 1 shows the appearance and the main composition of our head care robot. It is 810 mm wide, 723 mm long, 1045 mm high, and weighs approximately 100 kg. It consists of two main parts: a pair of swing arm units that scrub the front and top regions of the head and a rear unit that cleans its back (Fig. 1). Each swing arm unit consists of three main parts: an end effector that touches the head, a pressing arm that applies slight pressure to the head, and a shower pipe that sprays shampoo or water on the head.

An automatic shampooing machine that only uses a water stream has already been marketed in barber shops and hair salons [3][4][5]. However, it often gives people tickling or unpleasant sensations and consumes too much water (about 50 liters per use). Our head care robot can lightly scrub with its fingers and provides a lather of shampoo and a stream of water. It washes the hair more cleanly and only uses about 15 liters per shampoo.

III. Elemental Technologies

For a head care robot to wash hair instead of beauticians, the following are required: adapting to various head sizes and shapes, washing almost all of the head's hair, and satisfactorily both washing hair and supporting the head while keeping the body in a comfortable position. In this section, we introduce the main elemental technologies of our head care robot that addresses these requirements.

A. Multiple Contacts Driven by Cylindrical Rack Mechanism

For an end effector to have more than one contact point to softly touch the head with appropriate pressure, it needs to adapt to various head sizes and shapes. Although this can be done with multiple electric motors, we apply a cylindrical rack mechanism to the head care robot, and thus it only requires a single electric motor. A system with fewer actuators than degrees of freedom is called an underactuated mechanical system, many of which have been proposed and applied to robots in the past, for example, a connected differential mechanism [6] and a differential shaft mechanism [7]. The cylindrical rack mechanism used in head care robots resembles an underactuated mechanical system.

Fig. 2 shows the mechanism and motion of the end effector, which touches and lightly massages the head with eight soft rubber contacts like the fingers of a human hand. A self-aligning mechanism provides adaptable touches on the head, and a cylindrical rack mechanism permits only one electric motor to drive four self-aligned axes. We obtained a cylindrical rack shape by rotating the cross-section surface of a rack shape around the axis (A3).

Axes P1, P2, and P3 in Fig. 2(a) illustrate the types of passive joints used in the self-aligning mechanism. The end effector has seven passive joints: one P1 axis, two P2 axes, and four P3 axes. These axes are connected in a tree structure to allow three-dimensionally adaptable touches on surfaces with various curvatures and irregularities. This self-aligning mechanism is based on the average head shape of Japanese women developed by Kouchi[8]. The average head curvature radius is 76 mm, the assumed maximum head curvature radius is 110 mm, and the assumed minimum head curvature radius is approximately 56 mm. This indicates that the self-aligning mechanism can adapt to the head curvature radius of almost all Japanese men and women.

We installed a cylindrical rack mechanism in the end effector because its contacts need to be driven by a single electric motor through the passive joints of the self-aligning mechanism. The pinion gear (A1) shown in Fig. 2(a) is driven by an electric geared motor, and the motor's drive shaft (A2) is driven by this pinion gear. Two cylindrical racks (A3) are driven by the drive shaft (A2) and tentatively convert rotational motion into linear motion. Four gears (A4) are driven by two cylindrical racks (A3) to transform the linear motion back into rotational motion. Four gears (A5) are driven by four gears (A4), and eight contacts are driven by four gears (A5) through four passive joints (P3). Each cylindrical rack (A3) is arranged coaxially with a passive joint (P2) and can absorb the rotational displacement of a gear (A4) caused by a passive joint. This supports the self-aligning mechanism and allows the end effector to softly touch the head (Fig. 2(b)) and achieve an efficient driving-force transmission mechanism that uses only one electric motor (Fig. 2(c)).

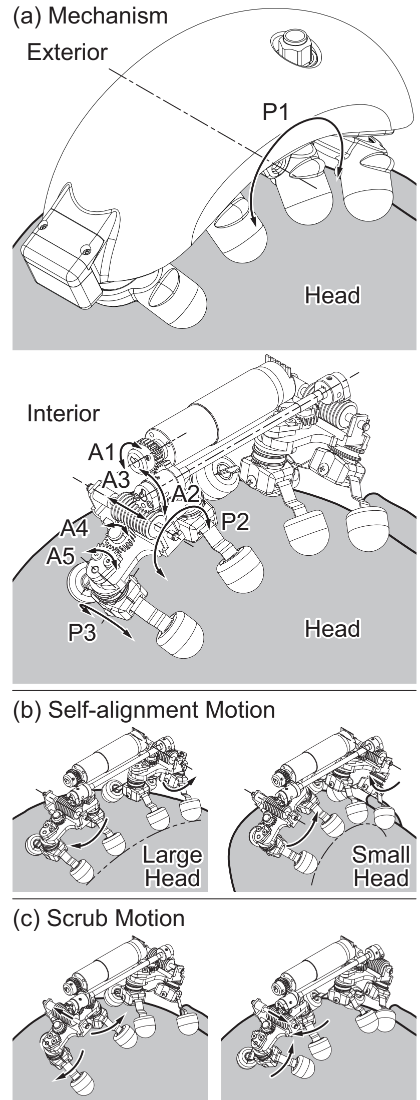

Fig. 2. End Effector Equipped with Self-aligning Mechanism and Cylindrical Rack Mechanism

B. Movement of Scrubbing Area by Five-bar Closed Link Mechanism

Movement of the scrubbing area is required to wash almost all of the head's hair. The hair-washing robot we developed previously [9] moved the scrubbing area by a swinging motion of the swing arm unit. Since the scrubbing area of each swing arm unit has no overlap, an area exists in the center that is shampooed by neither of the swing arm units. To solve this problem, we introduce a five-bar closed link mechanism into the robot's swing arm units and add one degree of freedom to each previous swing arm unit for a total of 4 DOFs. This allows each swing arm unit to realize extension motion and to alternately wash the cephalic area in the head's center.

The pressing arm supports the end effector and moves it on or off the head. Fig. 3 shows the mechanism and motion of the pressing arm. Even though the pressing arm actually has a

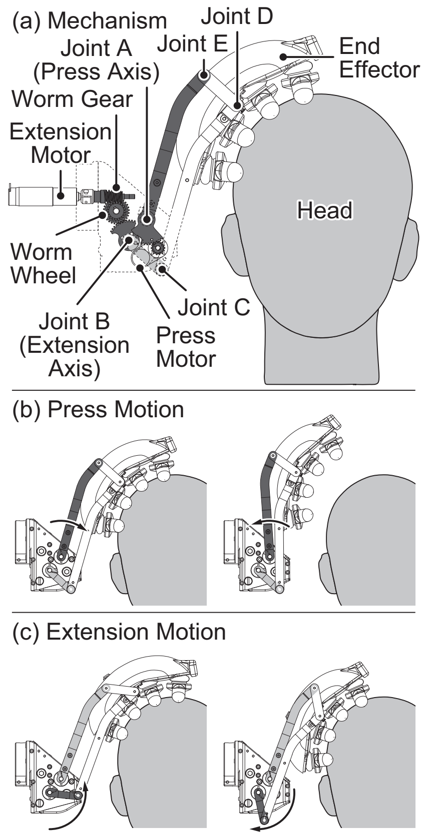

Fig. 3. Pressing Arm Equipped with Five-bar Closed Link Mechanism

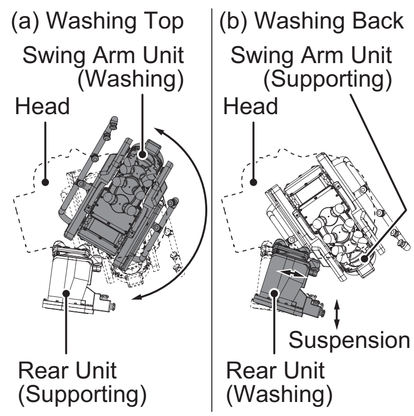

Fig. 5. Motion of Swing Arm and Rear Units

cover to prevent it from catching part of the head in it, Fig. 3 shows it without a cover for demonstration purposes. We put a five-bar closed link mechanism in the pressing arm and provided compliance control for the arm by measuring the pressing force with the force sensors described below. There are five joints (A to E) in the five-bar closed link mechanism, and five links are connected like a pentagon (Fig. 3(a)). The pressing arm realizes a press motion (Fig. 3(b)) by driving the press axis (joint A) by a press motor to move the end effector on and off the head. The pressing arm also realizes extension motion (Fig. 3(c)) by driving the extension axis (joint B) by an extension motor through a worm gear and a worm wheel to move the end effector to the center or the side of the head. About 34-cm extension motion is available that covers almost the entire hair area of the average head [8].

The pressing arm, as mentioned above, is controlled by the compliance control with force sensors attached to the passive axis (P1) shown in Fig. 2. A block diagram of the pressing arm's compliance control is shown in Fig. 4. Press angle (θ) indicates the angle of the press axis (joint A), extension angle (ϕ) indicates the angle of the extension axis (joint B), and extension length (r) indicates the length of the segment connecting joints A and D. We designed the regulator of the press motor based on the position control and the pressing force servo system using the output of force sensors (f). The extension angle converter calculates extension target angle (ϕ_{ref}) from extension target length (r_{ref}). Changing extension angle (ϕ) not only causes displacement in the direction of extension (r) but also in the direction of press (x_{int}). To reduce such interference, we designed a stabilizing decoupling compensator for the displacement in the direction of the press. It estimates the displacement in the direction of press ($\hat{x}_{int}$), and the results of multiplying estimated value ($\hat{x}_{int}$) by the inverse of estimated extension length ($\frac{1}{\hat{r}}$) are added to press target angle (θ_{ref}). This reduces the displacement in the direction of press (x_{int}) that is caused by changing extension angle (ϕ), and the variation of the press force error approximately decreases from 20 to 10%.

C. Press Force Control of Rear Unit by Coordinated Double Arm Motion

When the hair is being shampooed, the back of the head must be supported to keep the body in a comfortable position. If the robot also intends to wash the back of the head, it must simultaneously wash the hair and support the head. Therefore, our head care robot has a rear unit that can both shampoo the hair and support the head. When the rear unit shampoos the back of the head, a pair of swing arm units supports the top of the head and realizes press force control of the rear unit.

Fig. 5 shows the motion of a pair of swing arm units and the rear arm unit. The rear units support the back of the head when the pair of swing arm units swing and wash the front and top of the head (Fig. 5(a)). The pair of swing arm units supports the top of the head and reduces the press force of the rear unit when it swings and scrubs the back of the head (Fig. 5(b)). The rear unit has a suspension mechanism, which has no effect because of a stopper mechanism for cases of force overload when a pair of swing arm units wash the front and top regions of the head (Fig. 5(a)); it becomes effective when the rear unit washes the back of the head (Fig. 5(b)) by reducing the press force of the rear unit.

When the rear unit washes the back of the head, a pair of swing arm units makes a coordinated double arm motion to support the top of the head by controlling the rear unit's press force with force sensors, and the rear unit applies appropriate

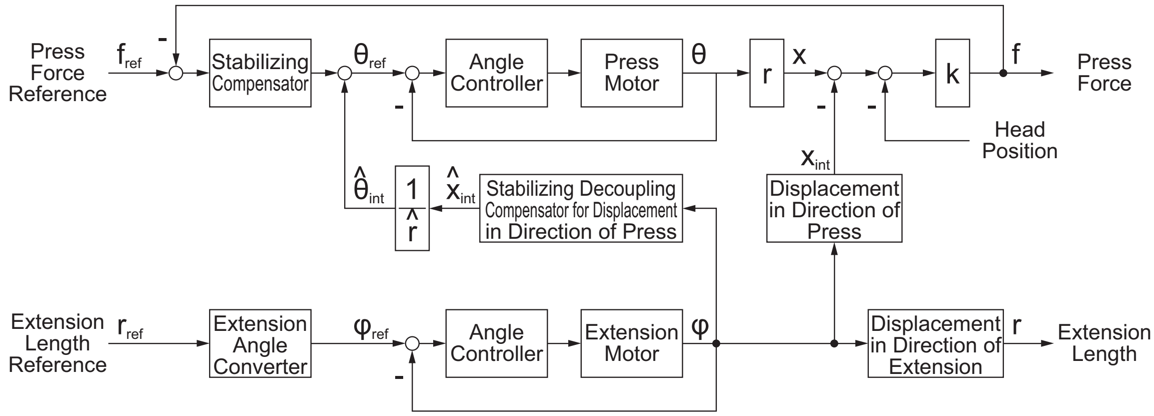

Fig. 4. Press Force and Extension Length Control of Pressing Arm

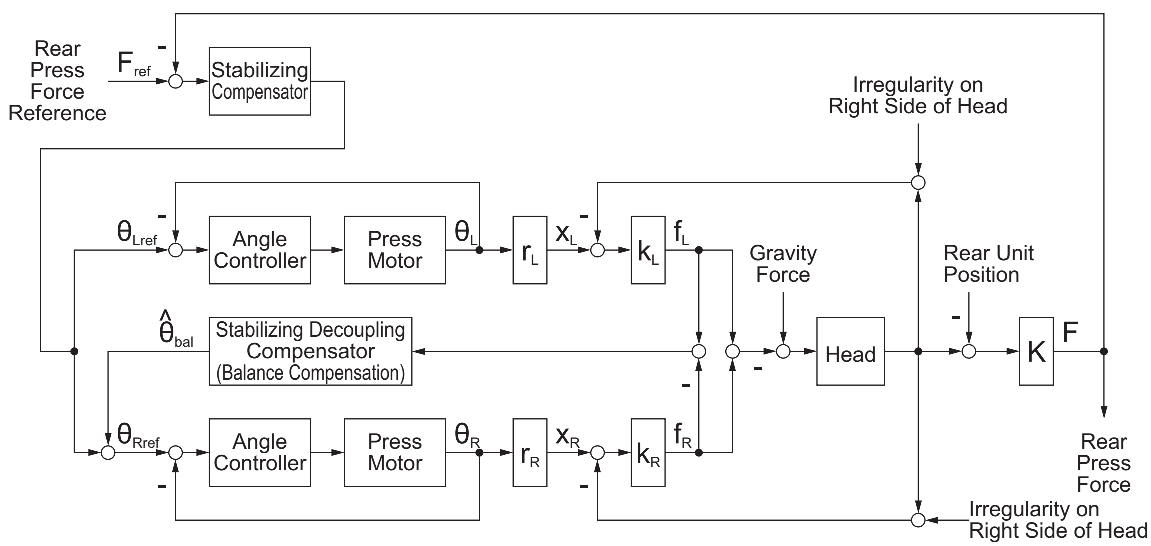

Fig. 6. Press Force Control of Rear Unit by Coordinated Double Arm Motion

pressure to the back of the head. Fig. 6 shows the press force control of the rear unit by the coordinated double arm motion of a pair of swing arm units.

The press motors in a pair of swing arm units are regulated by the PID angle controller. The force sensors in the rear unit detect its press force (F), and the target press angles of a pair of swing arm units (θ_{Lref}, θ_{Rref}) are controlled by the force servo system based on the press force of the rear unit (F). The difference of the shape of the left and right sides of the head creates an imbalanced motor load between the left and right motors of a pair of swing arm units; one may become overloaded. To equalize this imbalance, the difference value between the press forces of a pair of swing arm units (f_L and f_R) is added to target press angle (θ_{Rref}) to disperse the motor load on the left and right motors of a pair of swing arm units.

IV. Enhanced Head Shape Following Capability of Orientation Correction Mechanism

The five-bar closed link mechanism equipped in the pressing arm is introduced in section III-B and makes two motions: press and extension. However, the five-bar closed link mechanism raises a new problem concerning the end effector orientation: it can't keep the contact face of the end effector aligned along the head's surface when the end effector moves closer to the head. In this section, we introduce an orientation correction mechanism into our five-bar closed link mechanism to keep the contact face of an end effector aligned along the head's surface. We also explain the kinematics of the five-bar closed link mechanism and discuss improvements of the head shape following capability using an orientation correction mechanism.

A. Forward Kinematics of Five-bar Closed Link Mechanism

We define a point at the intersection of the symmetry plane of a pair of swing arm units with the rotational axis of the swing motion as original point O (Fig. 7). The coordinates of points A and B are defined as (x_A, y_A) and (x_B, y_B). The angles between segment AE and the x-axis and between segment BC and the x-axis are defined as θ_{AE} and θ_{BC}. The lengths of segments AE, BC, ED, and CD are respectively defined as L_{AE}, L_{BC}, L_{ED}, and L_{CD}. Table I shows the specifications of the five-bar closed link mechanism of our head care robot.

The coordinates of points E and C ((x_E, y_E) and (x_C, y_C)) are shown below using (x_A, y_A), (x_B, y_B), L_{AE}, L_{BC}, θ_{AE}, and θ_{BC}:

$$x_E = x_A + L_{AE}\cos\theta_{AE} \tag{1}$$
$$y_E = y_A + L_{AE}\sin\theta_{AE} \tag{2}$$
$$x_C = x_B + L_{BC}\cos\theta_{BC} \tag{3}$$
$$y_C = y_B + L_{BC}\sin\theta_{BC} \tag{4}$$

The lengths of segment EC (L_{EC}) and the angle between segment EC and x-axis (θ_{EC}) are shown below using (x_E, y_E) and (x_C, y_C):

$$L_{EC} = \sqrt{(x_C - x_E)^2 + (y_C - y_E)^2} \tag{5}$$
$$\cos\theta_{EC} = \frac{x_C - x_E}{L_{EC}} \tag{6}$$
$$\sin\theta_{EC} = \frac{y_C - y_E}{L_{EC}} \tag{7}$$

The lengths of segments EC, ED, and CD are respectively defined as L_{EC}, L_{ED}, and L_{CD}. Angle CED ($\theta_{\angle CED}$) is shown below using a cosine theorem:

$$\cos\theta_{\angle CED} = \frac{L_{EC}^2 + L_{ED}^2 - L_{CD}^2}{2L_{EC}L_{ED}} \tag{8}$$
$$\begin{aligned}\sin\theta_{\angle CED} &= \sqrt{1 - \cos^2\theta_{\angle CED}} \\ &= \sqrt{1 - \left(\frac{L_{EC}^2 + L_{ED}^2 - L_{CD}^2}{2L_{EC}L_{ED}}\right)^2}\end{aligned} \tag{9}$$

The coordinate of point D ((x_D, y_D)) is shown using a sine theorem:

$$\begin{aligned}x_D &= x_E + L_{ED}\cos(\theta_{EC} - \theta_{\angle CED}) \\ &= x_E + L_{ED}(\cos\theta_{EC}\cos\theta_{\angle CED} + \sin\theta_{EC}\sin\theta_{\angle CED}) \\ &= x_E + \frac{(x_C - x_E)(L_{EC}^2 + L_{ED}^2 - L_{CD}^2)}{2L_{EC}^2} + \\ &\quad \frac{(y_C - y_E)\sqrt{4L_{EC}^2L_{ED}^2 - (L_{EC}^2 + L_{ED}^2 - L_{CD}^2)^2}}{2L_{EC}^2}\end{aligned} \tag{10}$$

$$\begin{aligned}y_D &= y_E + L_{ED}\sin(\theta_{EC} - \theta_{\angle CED}) \\ &= y_E + L_{ED}(\sin\theta_{EC}\cos\theta_{\angle CED} - \cos\theta_{EC}\sin\theta_{\angle CED}) \\ &= y_E + \frac{(y_C - y_E)(L_{EC}^2 + L_{ED}^2 - L_{CD}^2)}{2L_{EC}^2} - \\ &\quad \frac{(x_C - x_E)\sqrt{4L_{EC}^2L_{ED}^2 - (L_{EC}^2 + L_{ED}^2 - L_{CD}^2)^2}}{2L_{EC}^2}\end{aligned} \tag{11}$$

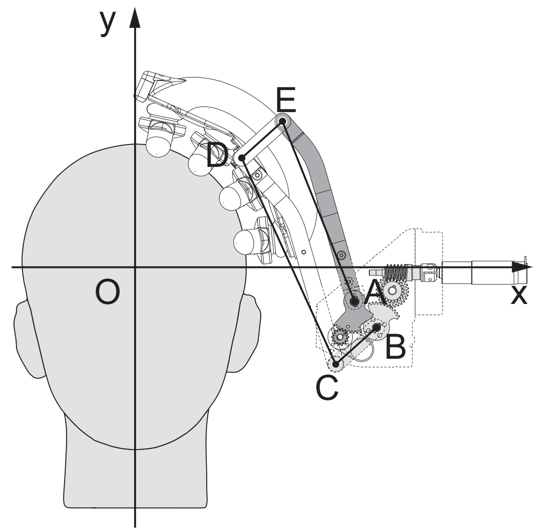

Fig. 7. Coordinate System Definition of Five-bar Closed Link Mechanism

TABLE I
SPECIFICATIONS OF FIVE-BAR CLOSED LINK MECHANISM

Item		Specification
Position of Press Axis	x_A	160 mm
	y_A	-25 mm
Position of Extension Axis	x_B	176 mm
	y_B	-44 mm
Angle of Press Axis	θ_{AE}	111.8^{+8}_{-23} °
Angle of Extension Axis	θ_{BC}	222 ± 39 °
Length of Link	L_{AE}	141.6 mm
	L_{BC}	40 mm
	L_{ED}	40 mm
	L_{CD}	165.3 mm

B. Inverse Kinematics of Five-bar Closed Link Mechanism

The lengths of segments AD and BD (L_{AD} and L_{BD}) and the angles between segment AD and the x-axis and between segment BD and the x-axis (θ_{AD} and θ_{BD}) are respectively shown using the coordinates of points A, B, and D ((x_A, y_A), (x_B, y_B) and (x_D, y_D)):

$$L_{AD} = \sqrt{(x_D - x_A)^2 + (y_D - y_A)^2} \tag{12}$$
$$L_{BD} = \sqrt{(x_D - x_B)^2 + (y_D - y_B)^2} \tag{13}$$
$$\tan\theta_{AD} = \frac{y_D - y_A}{x_D - x_A} \tag{14}$$
$$\tan\theta_{BD} = \frac{y_D - y_B}{x_D - x_B} \tag{15}$$

The lengths of segments AE and ED are defined as L_{AE} and L_{ED}. Angle EAD ($\theta_{\angle EAD}$) is shown by a cosine theorem:

$$\cos\theta_{\angle EAD} = \frac{L_{AE}^2 + L_{AD}^2 - L_{ED}^2}{2L_{AE}L_{AD}} \tag{16}$$
$$\begin{aligned}\tan\theta_{\angle EAD} &= \frac{\sqrt{1 - \cos^2\theta_{\angle EAD}}}{\cos\theta_{\angle EAD}} \\ &= \frac{\sqrt{4L_{AE}^2L_{AD}^2 - (L_{AE}^2 + L_{AD}^2 - L_{ED}^2)^2}}{L_{AE}^2 + L_{AD}^2 - L_{ED}^2}\end{aligned} \tag{17}$$

The lengths of the segment BC and CD are respectively defined as L_{BC} and L_{CD}. The lengths of segments BC and CD are defined as L_{BC} and L_{CD}. Angle ($\theta_{\angle CBD}$) is shown by a cosine theorem:

$$\cos\theta_{\angle CBD} = \frac{L_{BC}^2 + L_{BD}^2 - L_{CD}^2}{2L_{BC}L_{BD}} \tag{18}$$

$$\begin{aligned}\tan\theta_{\angle CBD} &= \frac{\sqrt{1-\cos^2\theta_{\angle CBD}}}{\cos\theta_{\angle CBD}} \\ &= \frac{\sqrt{4L_{BC}^2L_{BD}^2 - (L_{BC}^2 + L_{BD}^2 - L_{CD}^2)^2}}{L_{BC}^2 + L_{BD}^2 - L_{CD}^2}\end{aligned} \tag{19}$$

The angles between segment AE and the x-axis and between segment BC and the x-axis (θ_{AE} and θ_{BC}) are respectively shown by the addition theorem:

$$\begin{aligned}\tan\theta_{AE} &= \tan(\theta_{AD} - \theta_{\angle EAD}) \\ &= \frac{\tan\theta_{AD} - \tan\theta_{\angle EAD}}{1+\tan\theta_{AD}\tan\theta_{\angle EAD}}\end{aligned} \tag{20}$$

$$\begin{aligned}\tan\theta_{BC} &= \tan(\theta_{BD} + \theta_{\angle CBD}) \\ &= \frac{\tan\theta_{BD} + \tan\theta_{\angle CBD}}{1-\tan\theta_{BD}\tan\theta_{\angle CBD}}\end{aligned} \tag{21}$$

They are transcribed by inverse trig functions:

$$\begin{aligned}\theta_{AE} &= \pi + \tan^{-1}\frac{\tan\theta_{AD} - \tan\theta_{\angle EAD}}{1+\tan\theta_{AD}\tan\theta_{\angle EAD}} \\ &= \pi + \tan^{-1}\Big[\Big\{(y_D - y_A)(L_{AE}^2 + L_{AD}^2 - L_{ED}^2) \\ &\quad -(x_D - x_A)\sqrt{4L_{AE}^2L_{AD}^2 - (L_{AE}^2 + L_{AD}^2 - L_{ED}^2)^2}\Big\} \\ &\quad \Big/\Big\{(x_D - x_A)(L_{AE}^2 + L_{AD}^2 - L_{ED}^2) - (y_D - y_A) \\ &\quad \sqrt{4L_{AE}^2L_{AD}^2 - (L_{AE}^2 + L_{AD}^2 - L_{ED}^2)^2}\Big\}\Big]\end{aligned} \tag{22}$$

$$\begin{aligned}\theta_{BC} &= \pi + \tan^{-1}\frac{\tan\theta_{BD} + \tan\theta_{\angle CBD}}{1-\tan\theta_{BD}\tan\theta_{\angle CBD}} \\ &= \pi + \tan^{-1}\Big[\Big\{(y_D - y_B)(L_{BC}^2 + L_{BD}^2 - L_{CD}^2) \\ &\quad -(x_D - x_B)\sqrt{4L_{BC}^2L_{BD}^2 - (L_{BC}^2 + L_{BD}^2 - L_{CD}^2)^2}\Big\} \\ &\quad \Big/\Big\{(x_D - x_B)(L_{BC}^2 + L_{BD}^2 - L_{CD}^2) - (y_D - y_B) \\ &\quad \sqrt{4L_{BC}^2L_{BD}^2 - (L_{BC}^2 + L_{BD}^2 - L_{CD}^2)^2}\Big\}\Big]\end{aligned} \tag{23}$$

C. Installation of Orientation Correction Mechanism

Fig. 8(a) shows the orientation correction mechanism, which consists of five links (the base link and links AE, BC, ED, and CD) and three gears (gears L, M, and S). Gear L is arranged coaxially with joint E and fastened to link AE. Gear M can turn freely around the shaft on link ED and meshes with gear L. Gear S can turn freely around joint D and meshes with gear M. The end effector is connected to gear S through an elastic body and the end effector's orientation depends on that of gear S.

As the end effector moves closer to the head in both situations when the pressing arm is being extended or shortened, its motions are shown in Fig. 8(b) (with the orientation correction mechanism) and (c) (without the orientation correction mechanism). In the design before the orientation

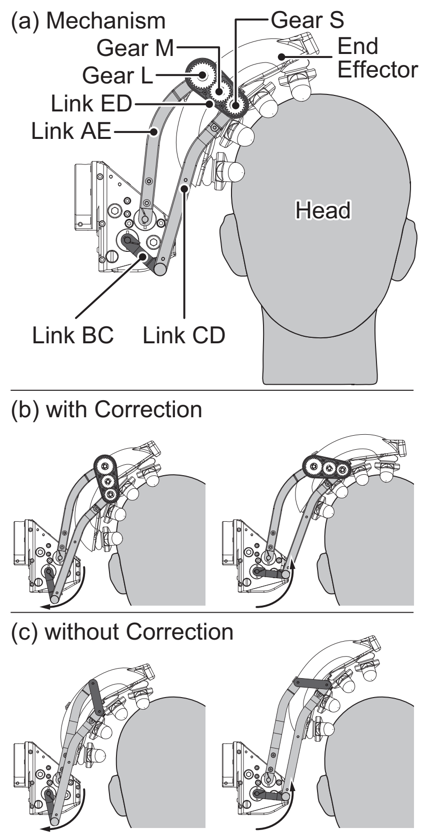

Fig. 8. Installation of Orientation Correction Mechanism

correction mechanism was installed, the end effector was connected to link CD through an elastic body, and its orientation depended on that of link CD. The two contacts nearest the ear touch the head first when the pressing arm is extended and the two contacts nearest the top of the head touch it first when the pressing arm is shortened when the end effector moves closer to the head (Fig. 8(c)). If the end effector continues to move closer to the head after the two contacts near the ear or the top of the head touch the head first, all of the contacts manage to touch the head because of the self-aligning mechanism of passive axis P1 in Fig. 2(b) and the elastic body connecting the end effector to link CD. However, in some cases, the friction force acting on the head and the two contacts touching the head first restrict all the contacts from touching the head.

In our design after installing the orientation correction mechanism, we connected the end effector to gear S through an elastic body and the end effector's orientation depended on that of gear S. All of the contacts touch the head almost at the same time in both the pressing arm extended and shortened situations when the end effector moves close to the head (Fig. 8(b)). This makes the self-aligning mechanism of passive axis P1 work more effectively.

The ratio of the relative change in the angle of link AE with respect to link ED (the relative change in angle AED: $\Delta\theta_{\angle AED}$) and the relative change in the angle of the end effector with respect to link ED can be determined by the

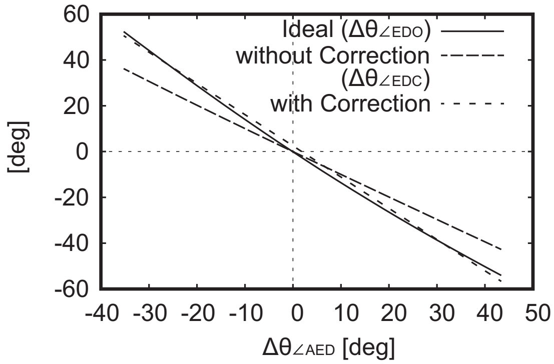

Fig. 9. Correction Angle Design of Orientation Correction Mechanism

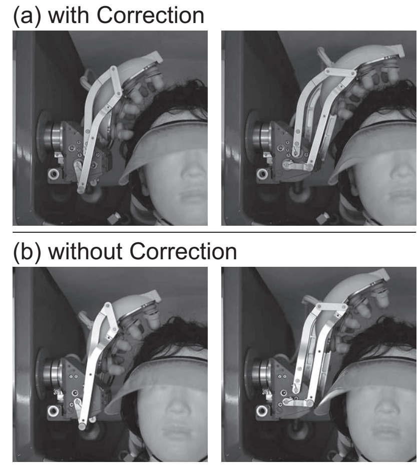

Fig. 10. Experiment of Orientation Correction Mechanism

gear ratio of gears L and S ($L : S$). A relative change in this section is determined as the difference from the reference state: press angle (θ_{AE}) is 111.8° and extension angle (θ_{BC}) is 222°.

We approximated the average head shape of Japanese women [8] by a 76-mm radius sphere. The ideal relation for the contact face to align an end effector along the head's surface is shown as a relative change in angle EDO ($\Delta\theta_{\angle EDO}$) plotted in Fig. 9. The relation before installing the orientation correction mechanism is shown as a relative change in angle EDC ($\Delta\theta_{\angle EDC}$) plotted in Fig. 9. There is an approximate difference of up to 16.2° between these two relative changes.

The linearly approximated relation of the ideal relation is shown as "with correction" in Fig. 9. The slope of the plotted line is $-15/11$ and is determined by the gear ratio of gears L and S ($L : S = 15 : 11$). The y-intercept of the plotted line is 2.5° and is determined by a change in the phase of link AE and gears L or S and the end effector. The difference from the ideal relation is approximately suppressed up to 2.6°.

We actually installed an orientation correction mechanism in the head care robot and experimentally assessed its effect. Fig. 10 shows the condition when one of the contacts of the end effector touches the head first. An orientation correction mechanism is installed behind the end effector in Fig. 10(a). All of the contacts touch the head almost at the same time in both situations when the pressing arm is extended or shortened after we installed the orientation correction mechanism (Fig. 10(a)). On the other hand, the two contacts nearest the ear touch the head first when the pressing arm is extended, and the two contacts nearest the top of the head touch it first when the pressing arm is shortened before we installed the orientation correction mechanism (Fig. 10(b)). This confirmed that our orientation correction mechanism works well, and we plan to evaluate subject satisfaction by adding it to our head care robot in the future.

V. Conclusions and Future Works

In this paper, we developed a head care robot equipped with scrubbing fingers and achieved the following mechanical and control technologies for gently touching the head:

- a cylindrical rack mechanism for self-aligning and a drive-force transmission from an electric motor to multiple fingers
- a five-bar closed link mechanism to expand the head's scrubbing area by extension motion
- rear pressure force control by coordinated double arm motion to switch between supporting and washing the head.

We also introduced an orientation correction mechanism into a five-bar closed link mechanism to keep the end effector's contact face aligned along the head's surface. We experimentally evaluated the orientation correction mechanism and concluded that it works well.

We are planning to improve our head care robot and make it more attractive. We also envision its practical use in hospitals and care facilities.

References

[1] V. Henderson: Basic Principles of Nursing Care, International Council of Nurses, 1997.

[2] F. Kazumi, K. Noriko, Y. Kana, and Y. Machio: "The Effects of Hair Shampooing as Nursing Care," *Miyagi University Nursing Review*, vol. 11, no. 1, pp. 21-26, 2008.

[3] T. Sakane and K. Kuroda: "Development of an Automatic Shampooer," *Sanyo Technical Review*, vol. 8, no. 1, pp. 45-53, 1976.

[4] "Automatic Shampooing Machine AQUAFORTE," *http://www.tb-net.jp/products/shampoo/aquaforte/*.

[5] "AUTO SHAMPOO Shampoo Lize III," *http://www.oohiro.ws/eg/products/002shampoo/v520.html*.

[6] S. Hirose, "Connected Differential Mechanism and Its Applications," *Proceedings of the 2nd International Conference on Advanced Robotics*, 1985.

[7] T. Tojo, A. Okuda, T. Tanimoto, O. Mizuno, and T. Nakamura, "Studies of a Lightweight Robot Hand using Differential Shaft Mechanisms," *Proceedings of the 25th Annual Conference of the Robotics Society of Japan*, 3M26, 2007.

[8] M. Kouchi and M. Mochimaru, Anthropometric Database of Japanese Head 2001, National Institute of Advanced Industrial Science and Technology, H16PRO-212, 2008.

[9] T. Hirose, S. Fujioka, O. Mizuno, and T. Nakamura, "Development of Hair-washing Robot Equipped with Scrubbing Fingers," *Proceedings of the 2012 IEEE International Conference on Robotics and Automation*, 2012.